Title

A MIRCROSCOPIC STUDY OF THE VARIABLE-MOMENT-OF-INERTIA MODEL FOR RARE EARTH NUCLEI

Authors

Ma, Chin W.
Tsang, Chin Fu.

Publication Date

1974-07-01

Submitted to Physical Review

LBL-2347
Preprint

A MIRCROSCOPIC STUDY OF THE VARIABLE-MOMENT-OF-INERTIA MODEL FOR RARE EARTH NUCLEI

Chin W. Ma and Chin Fu Tsang

July, 1974

Prepared for the U. S. Atomic Energy Commission
under Contract W-7405-ENG-48

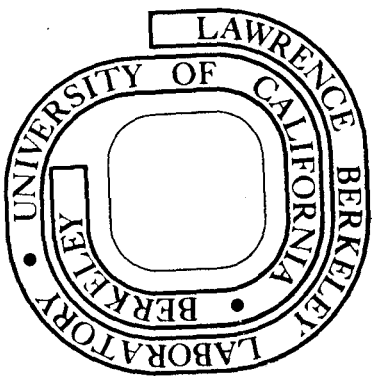

DISCLAIMER

LBL-2347

A MIRCROSCOPIC STUDY OF THE VARIABLE-MOMENT-OF-INERTIA MODEL FOR RARE EARTH NUCLEI*

Chin W. Ma+

Physics Department
Indiana University
Bloomington, Indiana 47401

and

Chin Fu Tsang

Lawrence Berkeley Laboratory
University of California
Berkeley, California 94720

July 1974

ABSTRACT

Based on the microscopic model, the moment-of-inertia parameter J_o and the force constant C_{VMI} associated with the variable-moment-of-inertia model are calculated microscopically for rare-earth nuclei Higher-order effects representing quadrupole and hexadecapole centrifugal stretching, proton and neutron Coriolis-anti-pairing effects and fourth-order cranking correction are included. The present calculations are able to reproduce the trend and the magnitude of both J_o and C_{VMI} fairly well with discrepancies ranging from 10 to 40 percent.

[NUCLEAR STRUCTURE rare earth even-even nuclei, calculated moment-of-inertia and force constant. Variable-moment-of-inertia model, cranking model. Coriolis-anti-pairing effect, fourth-order cranking, centrifugal stretching.]

I. INTRODUCTION

It is now well established that the quasi-rotational spectrum plays a central role in the excitations of even-even deformed nuclei.[1,2] The general features of the quasi-rotational states are as follows: 1) their spins and parities follow the sequence of 0^+, 2^+, 4^+, 6^+, . . ., and 2) their energies deviate from the $I(I+1)$ rule as the spins increase. Recently, it was discovered that at very high angular momenta, the rotational energies of some nuclei may exhibit anomalous behavior, the so called back-bending.[1,2,3] We shall not discuss the back-bending phenomenon in this paper, but shall limit our calculations only to those states with moderate high spins. There exist many two-parameter formulas which fit very well the energy levels up to spin $I\sim12$. Among them we may mention the centrifugal stretching model of Diamond, Stephens and Swiatecki[4] (which was later extended by Sood[5]), the fourth order cranking model of Harris[6], the variable moment-of-inertia model (VMI model) of Mariscotti, Scharff-Goldhaber and Buck[7], and the EXP model of Draper.[8] Recently the VMI model has also been extended to high spins by several authors to deal with the back-bending phenomenon.[9,10] Compared to the phenomenological fits, the microscopical calculations of the nuclear rotational energies,[11-17] on the other hand, have only moderate success in reproducing the experimental data. For example, the authors of Ref. 11 to Ref. 15 (Udagawa and Sheline; Chan and Valatin; Sano and Wakai; Bes, Landowne and Mariscotti; Krumlande) took into consideration the centrifugal stretching and the Coriolis-anti-pairing effect[18] (CAP effect) and obtained fairly good agreement with the experiment. However, other calculations[16,17] have shown that the fourth-order cranking contribution is as important as the CAP effect and the inclusion of the former makes the theoretical results much worse. Indeed, Marshalek's calculations[16] showed that in general the calculated

values of the B coefficient associated with the $I^2(I+1)^2$ correction term in an expansion of the rotational energies is about a factor of 1.5 to 3 too large compared with the experimental data in the rare-earth region. The calculations by Ma and Rasmussen[17] were likewise only capable to produce results of the right order of magnitude; however, the quantitative significance of their results is subject to some uncertainty due to the use of a simple basis where the single particle angular momentum is kept as a good quantum number. More recently, several authors[19-21] have done Hartree-Fock-Bogoliulov variational calculations to study the back-bending phenomenon at high spin states; which, however, will not be discussed here. In summary, the above situations indicate that the microscopic calculation of the rotational energy deserves much further study.

The present calculations are based on the cranking model of Inglis.[22] We follow closely the formulations of Ma and Rasmussen[17] (hereafter referred to as (I)), and make use of the single particle wave functions of Nilsson et al.[23] with the inclusion of both quadrupole (ε_2) and hexadecapole (ε_4) deformation. Since it has been shown that most of the two-parameter formulas are related to each other,[7,17,24] we shall calculate specifically the parameters associated with the VMI model and the B coefficient connected with the $I^2(I+1)^2$ term.

The following section will briefly review the formulations developed in (I), the detailed calculations and formulas are given in Sec. III, and the last two sections will give the results and discussions.

II. REVIEW OF MICROSCOPIC THEORY

The VMI model[7] can be expressed as follows:

$$\begin{cases} E_I = \frac{1}{2} C_{VMI} (J_I - J_O)^2 + \frac{I(I+1)}{2J_I} \\ \frac{\partial E_I}{\partial J_I} = 0 \end{cases} \tag{1}$$

where E_I and J_I are respectively the energy and moment-of-inertia of the excited state with spin I. The force constant C_{VMI} and the ground state moment-of-inertia J_o are the two parameters which can be determined by a least squared fit to the experimental energy levels. The VMI model is able to give very good fit for states up to spin I $\sim$ 12. Recently Saethre et al.[25] have improved the fitting by using a three-parameter and a four-parameter cranking model formulas. The two-parameter VMI model has been shown[7] to be mathematically identical to the Harris fourth order cranking model; in addition, Klein et al.[24] have proved that the VMI model and cranking model are equivalent to all orders.

The microscopic derivation of the VMI model has been given in (I) and will be briefly outlined below. One first expresses the total energy of a rotating system as

$$E = \sum_i \frac{1}{2} C_i (x - x_i)^2 + \frac{I(I+1)}{2J(x_i)} \tag{2}$$

where the potential energy is expressed approximately as a sum of harmonic terms each of which represents contributions from various collective degrees of freedom denoted here by x_i. C_i is the spring constant associated with

the i-th degree of freedom. The second term is the kinetic energy. The rotational solutions are obtained by minimizing Eq. (2) with respect to various x_i at a given value of spin I. In the present calculation we introduce as collective degrees of freedom the quadrupole and hexadecapole shape deformations ε_2 and ε_4 involved in the centrifugal stretching effect; the proton and neutron pairing correlation parameters ν_p and ν_n involved in the Coriolis-anti-pairing effect; and a new collective variable $\eta \equiv \omega^2$ involved in the fourth order cranking correction where ω is the angular velocity. Thus, we define (see (I) for details)

$$\{x_1, x_2, x_3, x_4, x_5\} \equiv \{\varepsilon_2, \varepsilon_4, \nu_p, \nu_n, \eta\} \tag{3a}$$

$$\{C_1, C_2, C_3, C_4, C_5\} \equiv \{C_{22}, C_{44}, C_{\nu p}, C_{\nu n}, C_\eta\} \quad . \tag{3b}$$

We have not included the asymmetric degree of freedom (gamma shape vibration), since its contribution is rather insignificant as was shown by the calculations of Marshalek.[16]

In the first order approximation, Eq. (2) can be reduced to Eq. (1) through a normal coordinate transformation and one obtains

$$C_{VMI}^{-1} = \sum_i \frac{1}{C_i} \left(\frac{\partial J(x_i)}{\partial x_i} \right)^2_{\{x_{io}\}} \tag{4}$$

where x_{io} is the value of x_i at the ground state, thus $\eta_o \equiv 0$. The moment-of-inertia $J(x_i)$ can be expressed as

$$J(x_i) = J_o(x_1, x_2, x_3, x_4) + 2\, C_\eta\, (x_1, x_2, x_3, x_4) \cdot \eta \quad . \tag{5}$$

The first term is the ground state moment-of-inertia which can be calculated by the well known cranking formula of Inglis[22] and Belyaev,[26]

$$J_o = 2\hbar^2 \sum_{m_\alpha > 0} \frac{|\langle \alpha' | j_x | \alpha \rangle|^2}{E_{\alpha'} + E_\alpha} (U_{\alpha'} V_\alpha - V_{\alpha'} U_\alpha)^2 \qquad (6)$$

where $|\alpha\rangle$ is the deformed single particle state with α denoting the appropriate quantum numbers, m_α is the magnetic quantum number along the symmetry axis, U_α and V_α are the probability amplitudes in the presence of pairing interaction and E_α is the quasi-particle energy.

The Inglis and Belyaev cranking formula (6) is based on the independent quasi-particle approximation. However, a recent calculation by Meyer, Speth and Vogeler[27] showed that the two carrection terms arising from the particle-particle and particle-hole interactions nearly cancel each other. It has also been shown by Rich[28] that correction due to particle-number conservation is also small. Thus it seems that the use of the cranking formula (6) is rather well justified numerically.

The second term of Eq. (5) represents the fourth order cranking correction which was first studied by Harris[6] and the fourth order cranking constant C_η can be expressed as[6]

$$C_\eta = 2 \sum_{m,n,p}{}' \frac{\langle \psi_o | J_x | \psi_m \rangle \langle \psi_m | J_x | \psi_p \rangle \langle \psi_p | J_x | \psi_n \rangle \langle \psi_n | J_x | \psi_o \rangle}{(\epsilon_m - \epsilon_o)(\epsilon_n - \epsilon_o)(\epsilon_p - \epsilon_o)}$$

$$-2 \sum_{m,n}{}' \frac{\langle \psi_m | J_x | \psi_o \rangle^2 \langle \psi_n | J_x | \psi_o \rangle^2}{(\epsilon_m - \epsilon_o)^2 (\epsilon_n - \epsilon_o)} \qquad (7)$$

where the ground state ψ_o is the quasiparticle vaccum state, ψ_m and ψ_n are two-quasiparticle states and the intermediate state ψ_p can be either two-quasiparticle or four-quasiparticle excitations. The corresponding energies are denoted by $\in_o$, $\in_m$, $\in_n$ and $\in_p$. The "prime" on the summation indicates that the ground state is excluded from the summation.

It is obvious from Eq. (5) that

$$\frac{\partial J}{\partial \eta} = 2C_\eta \quad .$$

Thus, the contribution of the fourth order cranking in Eq. (4) is simply $4C_\eta$ while the contributions of the other degrees of freedom are given by

$$\frac{1}{C_i}\left(\frac{\partial J_o}{\partial x_i}\right)^2_{\{x_{io}\}} \quad .$$

The B coefficient associated with the $I^2(I+1)^2$ term in the angular momentum expansion of the rotational energy

$$E_I = \frac{I(I+1)}{2J_o} + B\ I^2(I+1)^2 + C\ I^3(I+1)^3 + \ldots \tag{8}$$

can be expressed as

$$B = -\sum_i \frac{1}{8C_i J_o^4}\left(\frac{\partial J}{\partial x_i}\right)^2_{\{x_{io}\}} \quad . \tag{9}$$

The value of the force constant C_{VMI}^{-1} or the B coefficient indicates the degree to which the spectrum deviates from the I(I+1) rule. Both Eqs. (4) and (9) show that the contributions from various degrees of freedom are all positively added.

A simple relation between C_{VMI} and B can be obtained by combining Eq. (4) with Eq. (9), which yields

$$8\ B\ C_{VMI}\ J_o^4 = -1 \quad . \tag{10}$$

III. DETAILED CALCULATION AND FORMULAS

A. Single Particle Basis and the Pairing Problem

The deformed single particle basis used in the present calculations is chosen to be identical to that of Nilsson et al.[23] The diagonalization is carried out over the space of 11 shells for proton and 12 shells for neutron. The values of ε_2 and ε_4 of each nucleus are taken from the work of Nilsson et al. and are listed in Table I.

The pairing strength G is chosen to be a smooth function of A as suggested by Nilsson et al.

$$G \cdot A = g_o \pm g_1 \frac{N-Z}{A}$$

$$g_o = 19.2 \text{ MeV}$$

$$g_1 = 7.4 \text{ MeV} \tag{11}$$

with plus sign for protons and minus sign for neutrons. They also put in a linear surface dependence of G, which may be important for large deformation. The BCS equation is then solved by including $(15Z)^{1/2}$ or $(15N)^{1/2}$ states above and below the proton or neutron Fermi level. The pairing gap parameters Δ_p and Δ_n thus obtained are given in Table I.

The energy of a quasiparticle can be expressed as

$$E_k = (\varepsilon_k - \lambda)\ (U_k^2 - V_k^2) + 2U_k V_k\ G \sum_{\ell > 0} U_\ell V_\ell \qquad (12)$$

where ε_k is the single-particle energy and λ is the chemical potential. Following (I) we parametrize the probability amplitudes $\{U_k, V_k\}$ by introducing a pairing correlation parameter ν

$$\begin{matrix} U_k^2 \\ V_k^2 \end{matrix} = \frac{1}{2}\left[1 \pm \frac{\varepsilon_k - \lambda}{\sqrt{(\varepsilon_k - \lambda)^2 + \nu^2}}\right] . \qquad (13)$$

If $\nu = \Delta$ (the energy gap Δ is the equilibirium value of ν at ground state), Eq. (12) reduces to the familiar BCS result

$$E_k = \sqrt{(\varepsilon_k - \lambda)^2 + \Delta^2} . \qquad (14)$$

In what follows we shall vary ν to calculate the corresponding derivatives of moment-of-inertia as well as the pairing spring constant for a fixed pairing strength G as given by Eq. (11). Since for $\nu \neq \Delta$, the BCS gap equation no longer holds and Eq. (14) is not valid. Thus, it is important to use Eq. (12) rather than Eq. (14) as the expression for the quasiparticle energy.

B. Derivatives of the Moment-of-Inertia

We shall calculate the derivative of the moment-of-inertia J_o with respect to the pairing correlation parameter ν while the average particle number n and the pairing strength G are held fixed. One obtains

$$\left(\frac{\partial J_o}{\partial \nu}\right)_{n,G} = \left(\frac{\partial J_o}{\partial \nu}\right)_{\lambda,G} + \left(\frac{\partial J_o}{\partial \lambda}\right)_{\nu,G} \left(\frac{\partial \lambda}{\partial \nu}\right)_{n,G} \tag{15}$$

where J_o is given by Eq. (6) and the average particle number n is given by

$$\sum_{k>0} 2V_k^2 = n \quad . \tag{16}$$

It then follows

$$\left(\frac{\partial J_o}{\partial \nu}\right)_{\lambda,G|\nu=\Delta} = 2 \sum_{k,\ell} \frac{|\langle k|j_x|-\ell\rangle|^2}{E_k + E_\ell} (U_k V_\ell - U_\ell V_k) \quad .$$

$$\cdot \left\{ \begin{array}{l} (U_\ell^2 - V_\ell^2)(U_k U_\ell + V_k V_\ell)/E_\ell \\ - \dfrac{2U_\ell V_\ell (U_k V_\ell - V_k U_\ell)}{E_k + E_\ell} \cdot \dfrac{G}{\Delta} \sum\limits_{m>0} U_m V_m (U_m^2 - V_m^2)^2 \end{array} \right\} \tag{17a}$$

$$\left(\frac{\partial J_o}{\partial \lambda}\right)_{\nu,G|\nu=\Delta} = 2 \sum_{k,\ell} \frac{|\langle k|j_x|-\ell\rangle|^2}{E_k + E_\ell} (U_k V_\ell - U_\ell V_k) \cdot$$

$$\cdot \left\{ \begin{array}{l} 2U_\ell V_\ell (U_k U_\ell + V_k V_\ell)/E_\ell \\ + \dfrac{(U_k V_\ell - U_\ell V_k)}{E_k + E_\ell} \left[(U_\ell^2 - V_\ell^2) - 4U_\ell V_\ell \dfrac{G}{\Delta} \sum\limits_{m>0} U_m^2 V_m^2 (U_m^2 - V_m^2) \right] \end{array} \right\} \tag{17b}$$

$$\left(\frac{\partial \lambda}{\partial \nu}\right)_{n,G} = - \sum_{k>0} U_k^2 V_k^2 (U_k^2 - V_k^2) \Big/ 2 \sum_{k>0} U_k^3 V_k^3 \tag{17c}$$

Note that in taking the derivative, the quasiparticle energy is given by Eq. (12). After the derivative is taken, its value at $\nu = \Delta$ is then evaluated.

The derivatives of J_o with respect to the deformation parameters ε_2 and ε_4 are calculated by finite differences. The mesh point interval is taken to be 0.02 for both ε_2 and ε_4.

The various derivatives of the moment-of-inertia are listed in Table II. The derivative with respect to pairing are quite stable over the rare-earth region of nuclei. For example, with respect to the neutron pairing, the derivatives fluctuate around $-(36 \pm 10)$ MeV^{-2}, while the derivatives with respect to proton pairing are roughly equal to $-(19 \pm 3)$ MeV^{-2} for nuclei in the region of $A \sim 165$ and $-(11 \pm 2)$ MeV^{-2} for those in the region of $A \sim 187$. The derivatives with respect to the deformation, on the other hand, are quite different as one goes from one nucleus to another. In the case of quadrupole deformation (ε_2), the derivatives are largest at the beginning of the rare-earth region and generally decrease towards the end of the region; while in the case of hexadecapole deformation (ε_4), the derivatives are strongly negative at the beginning of the rare-earth region and change to positive values near the end. A negative value for the inertia derivative with respect to hexadecapole deformation (ε_4) has some interesting consequences. The equilibrium value of ε_4 at a given spin I in first order approximation is given in (I) as

$$\varepsilon_4 = \varepsilon_{40} + \frac{I(I+1)}{2C_{44}J^2} \frac{\partial J}{\partial \varepsilon_4} \qquad (18)$$

where ε_{40} is the hexadecapole deformation at ground state. In the beginning

of the rare-earth region, the values of both ε_{40} and the inertia derivative with respect to ε_4 are negative, thus, as the spin goes up, the hexadecapole deformation will increase in magnitude which is just the familiar stretching effect. However, for nuclei in the middle of the rare-earth region, the values of ε_{40} become positive while in most cases the inertia derivatives with respect to ε_4 still remain negative. Thus, as the spin goes up, the hexadecapole deformation will actually decrease.

Equilibrium values of quadrupole deformation ε_2 and of pairing parameters ν_p and ν_n at a given spin I can also be determined by equations similar to Eq. (18) which then yield the quadrupole stretching and the Coriolis-anti-pairing effect.

C. Pairing Spring Constant

The ground state energy can be expressed as

$$\in_o = \sum_{k>0} \varepsilon_k 2V_k^2 - G\left(\sum_{k>0} U_k V_k\right)^2 - G \sum_{k>0} V_k^4$$

$$-G \sum_{k\neq\ell>0} U_k V_k^3 U_\ell^3 V_\ell \Big/ \sum_{k>0} U_k^2 V_k^2 \qquad (19)$$

where the first three terms are the BCS ground state energy, and the last term approximately accounts for the fixed-particle-number correction.[29,30] The pairing spring constant C_ν can be obtained by taking the second derivative of $\in_o$ with respect to the pairing correlation parameter ν

$$C_\nu = \left(\frac{\partial^2 \in_o}{\partial \nu^2}\right)_{n,G}$$

$$= \left(\frac{\partial^2 \epsilon_o}{\partial \nu^2}\right)_\lambda + 2\left(\frac{\partial^2 \epsilon_o}{\partial \lambda \partial \nu}\right)\left(\frac{\partial \lambda}{\partial \nu}\right)_n + \left(\frac{\partial^2 \epsilon_o}{\partial \lambda^2}\right)_\nu \left(\frac{\partial \lambda}{\partial \nu}\right)_n^2$$

$$+ \left(\frac{\partial \epsilon_o}{\partial \lambda}\right)_\nu \left(\frac{\partial^2 \lambda}{\partial \nu^2}\right)_n \quad . \tag{20}$$

Evaluation of the derivatives of ϵ_o with respect to λ and ν are straightforward by using Eq. (19). The derivative of λ with respect to ν can also be easily obtained in terms of Eq. (16). The proton and neutron pairing spring constants $C_{\nu p}$ and $C_{\nu n}$ as calculated by Eq. (20) are given in Table III.

It is interesting to note that inclusion of the fixed-particle-number correction in the ground state energy will in general increase the pairing spring constant by about 20 percent, hence, reduces the CAP effect. Some of the examples are given in Table IV.

A simple formula for C_ν based on the continuous model is given in (I) which reads

$$C_\nu = (2\rho + \frac{2}{\pi\Delta})\ (1 - \rho\, G) \tag{21}$$

where ρ is the average nucleon orbital level density. The spring constant given by Eq. (21) (see Table I of (I)) are somewhat larger than those given by the present calculations by about 5 to 15 percent in the case of proton and 10 to 25 percent in the case of neutron. In view of the tremendous numerical work involved in Eq. (20), the simple formula Eq. (21) is indeed a very useful approximation.

D. Shape Spring Constant

The shape spring constants C_{22} and C_{44} associated with the quadrupole ε_2 and hexadecapole ε_4 deformation degrees of freedom can be obtained similarly by taking the second derivative of the ground state energy $\in_o$ with respect to ε_2 and ε_4

$$C_{22} = \frac{\partial^2 \in_o}{\partial \varepsilon_2^2} \ , \ C_{44} = \frac{\partial^2 \in_o}{\partial \varepsilon_4^2} \quad . \tag{22}$$

In applying Eq. (22), the ground state energy $\in_o$ is calculated according to the Strutinsky average prescription as described in Ref. 23 by Nilsson et al. The C_{22} and C_{44} are then obtained by finite differences with the mesh point interval taken to be 0.02 both for ε_2 and ε_4; the results are listed in Table III.

The curvatures C_{22} and C_{44} at the ground state deformation are due to contributions from the liquid drop energy part, the shell correction part and the pairing energy part, which make up the potential energy surface. The shell correction part gives the largest positive contirbution and in fact determines, to the larger extent, the deformation of the ground state nucleus. The pairing effect tends to smooth out the level density and thus acts against the shell effect. It provides a negative contribution to the curvature. The liquid drop energy part in general gives a small positive contribution.

The Strutinsky normalization replaces the smooth part of the eigen-energy summation by the liquid drop energy. Due to the inadequacy of volume normalization of the single particle potential well, the former has a much stronger curvature than that of the liquid drop part, as is obvious from the fact that its value would be infinite at $\varepsilon = 1.5$ (which is of course quite far

away from the ground state deformation of $\varepsilon \sim 0.25$), whereas the liquid drop energy would be finite. Hence, one would expect the value of curvature calculated in a scheme with the employment of Strutinsky normalization to be smaller than the value calculated without it. This is indeed borne out by our detailed calculation which show that the Strutinsky normalization generally reduces the values by about 20 percent.

On comparison with Table I of (I), our present results for C_{22} are about 40 to 100 percent larger. The first reason is that we are currently using a finer set of grids, $\Delta\varepsilon = 0.02$, as compared with $\Delta\varepsilon = 0.05$ used in the older calculation. Thus, the new calculations are less likely to suffer from the problem of anharmonic effects in the potential energy surface which, in the present case, will tend to reduce the effective value of the curvature. The second and probably the main reason behind the discrepancy is that the older calculation used a surface-independent pairing force; whereas the new calculation has a pairing force dependent on the surface area. For most properties of the nucleus near the ground state, this difference does not present significant discrepancy. But for such higher-order effect as the curvature, we find it does make a difference. When we calculated the pairing energy contribution, we found that the new calculation with a surface-dependent pairing force gives a smaller negative value than the old calculation, and the change is sufficient to account for the discrepancy between the two results. A detailed discussion was made by other authors[23,34] on the choice of these two versions of the pairing force. We have not pursued the question regarding which is the more appropriate form of pairing force to be used. However, as will be seen later, the contribution of centrifugal stretching effect to the VMI

force constant is very small when compared with the contributions from Coriolis-anti-pairing and fourth-order cranking effect, so that either choice of the pairing force will have little effect on our final results and conclusions.

E. Fourth Order Cranking Constant C_η

The evaluation of the fourth order cranking constant C_η given by Eq. (7) is rather tedious, since now one has to calculate the contributions from the four-quasiparticle intermediate states as well as those from the two-quasiparticle states. Fortunately, we are able to reduce Eq. (7) to a sum of quadratic terms; as a resut, the numerical work is considerably simplified. We shall quote the final result below while the derivation will be given in the appendix.

$$C_\eta = -4 \sum_{\substack{m_p \rangle 0 \\ m_q = m_p - 1 \\ m_{q'} = m_p + 1}} \sum_{t_q, t_{q'}} (E_q + E_{q'}) \cdot$$

$$\cdot \left[\sum_{t_p} \langle p|j_x|q\rangle \langle p|j_x|q'\rangle \frac{(U_p V_q - V_p U_q)\ (U_p V_{q'} - U_{q'} V_p)}{(E_p + E_q)\ (E_p + E_{q'})} \right]^2$$

$$-2 \sum_{m_p = m_{p'} \rangle 0} \sum_{t_p, t_{p'}} (E_p + E_{p'}) \cdot$$

$$\cdot \left[\sum_{\substack{t_q \\ m_q = m_p \pm 1}} \frac{\langle p|j_x|q\rangle \langle p'|j_x|q\rangle\ (U_p V_q - V_p U_q)\ (U_{p'} V_q - V_{p'} U_q)}{(E_p + E_q)\ (E_{p'} + E_q)} \right]^2 +$$

$$+4 \sum_{\substack{m_p \rangle 0 \\ m_q = m_p - 1 \\ m_{q'} = m_p + 1}} \sum_{t_q, t_{q'}} \frac{1}{E_q + E_{q'}} \left\{ \sum_{t_p} \langle p|j_x|q\rangle\langle p|j_x|q'\rangle \cdot \right.$$

$$\left. \cdot \left[\frac{(U_p V_q - V_p U_q)(U_p U_{q'} + V_p V_{q'})}{E_p + E_q} + \frac{(U_p V_{q'} - V_p U_{q'})(U_p U_q + V_p V_q)}{E_p + E_{q'}} \right] \right\}^2$$

$$+2 \sum_{m_p = m_{p'} \rangle 0} \sum_{t_p, t_{p'}} \frac{1}{E_p + E_{p'}} \cdot$$

$$\cdot \left\{ \sum_{\substack{t_q \\ m_q = m_p \pm 1}} \langle p|j_x|q\rangle\langle p'|j_x|q\rangle \cdot \right.$$

$$\left. \cdot \left[\frac{(U_p V_q - V_p U_q)(U_{p'} U_q + V_{p'} V_q)}{E_p + E_q} + \frac{(U_{p'} V_q - V_{p'} U_q)(U_p U_q + V_p V_q)}{E_{p'} + E_q} \right] \right\}^2 \qquad (23)$$

where m_p is the magnetic quantum number of the particle in state $|p\rangle$, t_p denotes the quantum numbers other than m_p and E_p is the corresponding quasi-particle energy. The first two terms represent the contributions from four-quasiparticle intermediate states while the last two terms represent those from two-quasiparticle intermediate states, as can readily be seen from the form of the products of the U, V coefficients. The fourth order cranking constants

C_η calculated in terms of Eq. (23) are listed in Table III. Our calculations show that the two-quasiparticle contribution is always positive while the four-quasiparticle contribution is always negative. Furthermore, the former is generally about three to four times larger than the latter in magnitude. Some of the examples are given in Table IV.

IV. RESULTS AND DISCUSSIONS

A. Moment-of-Inertia

The ground state moment-of-inertia J_o is calculated according to Eq. (6). In addition, we have followed Nilsson and Prior[31] and increased the calculated values by 5 percent which represents approximately the effects of the coupling between the shells N and N + 2, due to the j_x operator. This is because the Nilsson wave functions of Ref. 23 are expressed in the stretched coordinates and the j_x operator in these stretched coordinates will give rise to a term which will couple the shells N and N + 2. The results are listed in Table II and plotted in Fig. 1. From Fig. 1, it is seen that the trends of the experimental moment-of-inertia are well reproduced by the calculations. The calculated magnitudes, however, are generally too small by 10 to 40 percent, the average discrepancy being 25 percent. This disagreement in magnitude seems to be somewhat too large compared to a similar calculation by Nilsson and Prior[31] where the calculated J_o are generally 10 to 30 percent too small, the average discrepancy being 20 percent. But it should be pointed out that in the present calculation, the single particle states and the parameters G, ε_2, ε_4 are all taken directly from the works of Nilsson et al.[23] without any readjustment. One may, for example, obtain very good agreement with the experimental data by choosing g_o = 18.0 MeV instead of 19.2 MeV in Eq. (11). We shall return to this question at the end of this section.

B. Force Constant C_{VMI}

The force constant C_{VMI}^{-1} associated with the VMI model of Eq. (1) is calculated using Eq. (4) and the results are listed in Table V and plotted in Fig. 2. The contributions to C_{VMI}^{-1} from various sources are also given

separately in Table V. One notices first that except for nuclei with neutron number N = 90 and 92, both quadrupole and hexadecapole centrifugal stretching contribute very little to the energy deviation from the I(I+1) rule. Typically they amount to only a few percent of the total contribution and hence in most cases can be entirely neglected. This result is consistent with other microscopic calculations and also with experimental observations.[32] It is important to note that the contributions of hexadecapole stretching are comparable with those of quadrupole stretching. Hence they should both be taken into account in other relevant analyses, such as the study[16] of change of nuclear mean-square radius $\Delta \langle r^2 \rangle$ or the study of the deviation of the transition probability from the rigid rotor formula.

It is shown in Table V that the neutron Coiolis-anti-pairing and the fourth-order cranking corrections are the two largest contributions and are comparable with each other. The proton Coriolis-anti-pairing term is relatively smaller and amounts to about 10 to 20 percent of the total contribution. In general, the present results are very different quantitatively from those of (I). However, many qualitative discussions of (I) are still valid.

We observe in Fig. 2 that except for nuclei with neutron number N = 90, 104 and 108, both the experimental trend and magnitude of the force constant C_{VMI}^{-1} are fairly well reproduced in general by the present calculation. In most cases the discrepancy ranges from 10 to 40 percent; the average discrepancy for all nuclei (excluding those with N = 90) is about 34 percent.

The large discrepancies of the calculated force constants which occurred at neutron number N = 90, 104 and 108 deserve more careful study. Perhaps the 90-neutron nuclei are so close to being shape unstable that the present model of stable deformation may be somewhat questionable. This argument, however, cannot be applied to nuclei with N = 104 and 108, all of which appear to be good rotors. We then compare the calculated Nilsson single neutron levels aroung N = 104 and 108 with those deduced semi-empirically by Ogle et al.[33] and are not surprised to find some discrepancies between them. Consequently, we make the following preliminary neutron level shifts

$$\text{Calculation B:} \begin{cases} [512,\ 5/2^-]_n + 0.05\ \hbar\omega \\ [510,\ 1/2^-]_n - 0.05\ \hbar\omega \quad \text{for } A \geqslant 170 \\ [512,\ 3/2^-]_n - 0.05\ \hbar\omega \end{cases} \tag{24}$$

With the above neutron level shifts and assuming further that the wave function and the quadrupole and hexadecapole stretching are the same, we repeat the calculation on the moment-of-inertia and the force constant which will be called calculation B while the previous calculation without level shifts will be called calculation A. The results of calculation B are listed in Table VI. In general, the results of calculation B are similar to those of calculation A except for nuclei around neutron number N = 104 and 108. Note in Table VI that the moments-of-inertias from calculation B change only slightly over the results of calculation A. On the other hand, the force constants of calculation B are considerably improved over the results of calculation A around N = 104 and 108, as can be seen in Fig. 3. The serious discrepancies of calculation A which occurred at N = 104 and 108 are now much reduced; in most cases, both the trend and magnitude of the

experimental force constants are now fairly well reproduced. However, in addition to the 90-neutron nuclei there still remain three nuclei ($^{170}_{102}Er$, $^{174}_{104}Yb$ and $^{180}_{108}Hf$) whose calculated force constants are a factor of 2 too large compared to the experiment. The average discrepancy for all nuclei (excluding N = 90) is now 29 percent. Thus the agreement between the theoretical and experimental values of the force constant is comparable to that of the moment-of-inertia calculations.

The above results indicate that the force constant C_{VMI} which represents the higher-order effects in the rotational energy calculation is much more sensitive to the single particle levels than the moment-of-inertia. We have no intention here to do a detailed searching for better single neutron levels. Instead, the emphasis is to indicate that by removing the discrepancy of the Nilsson neutron levels aroung N = 104 and 108 (although only in a preliminary way), the calculated results of the force constant C^{-1}_{VMI} can be considerably improved.

C. B Coefficients

The B coefficient associated with the $I^2(I+1)^2$ term in an expansion of the rotational energy can be evaluated either by Eq. (9) or in a more straightforward way, since we already know J_o and C^{-1}_{VMI}, by Eq. (10). The results of calculation B are given in Table VI and plotted in Fig. 4. The "experimental B coefficients are obtained by a least-squared-fit to the first three excited states by using the first three terms in Eq. (8) with J_o taken from Ref. 7. It is seen in Fig. 4 that the trend of the B coefficient is fairly well reproduced; the calculated magnitudes, however, are generally too large by a factor of 2 to 5. Thus, the agreements are much worse than those of the force constant C^{-1}_{VMI} although both of them represent the higher-order effects. The reason is easy to understand, because the B coefficient depends on the

inverse fourth power of the moment-of-inertia J_o according to Eq. (10). Our calculated J_o are roughly 10 to 40 percent smaller while our calculated C_{VMI}^{-1} are roughly 10 to 40 percent larger; so combined they yield the B values by a factor 2 to 5 too large.

Because of this J_o^{-4} dependence, it seems that in order to get reasonable agreement for B coefficient one probably should first fit the moment-of-inertia as accurately as possible. We have mentioned in the beginning of this section that very good agreements of the moment-of-inertia could be achieved provided one uses a reduced pairing strength g_o = 18.0 MeV instead of 19.2 MeV in Eq. (11). The values of J_o, B and C_{VMI}^{-1} calculated with g_o = 18.0 MeV and without neutron levels shifts are listed in Table VII. In addition, the second set of results of J_o and B of Marshalek[16] which are obtained by adjusting the pairing strength so as to exactly reproduce the experimental moment-of-inertia are also included for comparison. Our results are roughly similar to those of Marshalek at the middle of the rare-earth region, though discrepancies occur at both ends of this region. Note also in Table VII that our B values are now improved over those obtained previously with g_o = 19.2 MeV, although they are still too large by a factor of 1.5 to 3 in general. On the other hand, however, the force constants C_{VMI}^{-1} in Table VII are much worse than those obtained previously with g_o = 19.2 MeV.

We seem to be in a very interesting situation. On the one hand, our calculation with pairing strength g_o = 19.2 MeV is able to reproduce fairly well J_o and C_{VMI}; however, it yields very poor B coefficients. On the other hand, very good J_o and improved values of B (but still too large by a factor of 1.5 to 3) could be obtained from calculation with the reduced pairing

strength g_o = 18.0 MeV, but now the C_{VMI} becomes very poor. We feel that an accurate microscopic theory should be able to reproduce both force constant and the B coefficient correctly. For calculations involving as many approximations as these, however, we suggest that the force constant C_{VMI} is a more meaningful quantity to be compared with. The reasons are as follow: 1) Because of the J_o^{-4} dependence, the large discrepancy of the calculated B coefficient may be misleading since it may essentially be a result of small to moderate deviation in J_o. It is also probably misleading for one to obtain better B coefficient by adjusting the pairing strength alone in order to reduce the error arising from the J_o^{-4} dependence, because in doing so, the force constnat C_{VMI} will become unduly worse. 2) It is well known that the expansion of the rotational energy in terms of the angular velocity ω^2 is much better than the expansion in terms of the angular momentum I(I+1). Thus, the force constant C_{VMI} also appears to be a more physically significant parameter than the B coefficient.

V. SUMMARY

Based on the microscopic cranking model, the present calculations are able to reproduce fairly well the moment-of-inertia J_o and the force constant C_{VMI} associated with the VMI model with discrepancy ranging from 10 to 40 percent in general. On the other hand, the calculated B coefficients are quantitatively poor, which resemble the calculations of Marshalek.[16] However, as we have mentioned, one must use care in interpreting the large discrepancy of the B coefficient because of its J_o^{-4} dependence.

We have taken into account the fixed-particle-number correction for the potential energy; obviously it will also affect the moment-of-inertia and the fourth order cranking calculations. According to the calculation of Rich,[28] the fixed-particle-number correction will reduce the inertia derivative with respect to pairing by 10 to 20 percent. Since the force constant C_{VMI}^{-1} is proportional to the square of the inertia derivative, this will cause 20 to 50 percent reduction of the Coriolis-anti-pairing effect, which is in the right direction of improvement. We feel that the present approach is not accurate enough to study nuclear rotation at very high spin; to do that, the perturbation treatment on ωJ_x probably will have to be avoided altogether.

ACKNOWLEDGMENTS

We are grateful to S. Y. Chu for helpful descussions and for assistance in numerical calculations, and to J. O. Rasmussen for many valuable suggestions. We also wish to thank J. O. Rasmussen and J. Meyer ter Vehn for critical reading of the manuscript.

APPENDIX

We first express the J_x operator in the quasi-particle representation as

$$J_x = J_{11} + J_{20} \tag{A.1}$$

with

$$\langle p|J_{11}|q\rangle = \langle p|j_x|q\rangle (U_pU_q + V_pV_q) \tag{A.2a}$$

$$\langle o|J_{20}|pq\rangle = (-1)^{m_q+\frac{1}{2}} \langle p|j_x|-q\rangle (U_pV_q - V_pU_q) \tag{A.2b}$$

where $|0\rangle$ is the quasi-particle vacuum state. Note that J_x only operates between states with J_z components differed by ± 1.

Consider now the contribution of the four-quasiparticle excitations to the first term in Eq. (7)

$$C'_\eta(4QP) = 1/8 \cdot 2 \sum_{\substack{(pq)\pm 1 \\ (p'q')\pm 1 \\ (p_1q_1)\pm 1 \\ p\neq q\neq p'\neq q'}} \frac{\langle o|J_{20}|pq\rangle}{(E_p+E_q)} \times$$

$$\times \frac{\langle pq|J_{20}|pq,\ p'q'\rangle \langle pq,p'q'|J_{20}|p_1q_1\rangle \langle p_1q_1|J_{20}|o\rangle}{(E_p+E_q+E_{p'}+E_{q'})(E_{p_1}+E_{q_1})}$$

where $(pq)\pm1$ denotes a complete set of two-quasiparticle states $|pq\rangle$ with J_z component $m_p+m_q = \pm1$. Since for each $|pq\rangle$ there is a corresponding state $|qp\rangle$, the factor 1/8 thus accounts for the double counting of pq, $p'q'$ and p_1q_1. Writing the non-zero terms of the above expression explicitly one obtains

$$C'_\eta(4QP) = \tfrac{1}{2}\sum_{\substack{(pq)\pm1\\(p'q')\pm1\\p\neq q\neq p'\neq q'}} \left\{ \frac{\langle o|J_{20}|pq\rangle^2 \langle o|J_{20}|p'q'\rangle}{(E_p+E_q)^2 (E_{p'}+E_{q'})} \right.$$

$$- \frac{\langle o|J_{20}|pq\rangle \langle o|J_{20}|p'q'\rangle \langle o|J_{20}|pq'\rangle \langle o|J_{20}|p'q\rangle}{(E_p+E_q)(E_p+E_{q'})(E_{p'}+E_q)}$$

$$\left. - \frac{\langle o|J_{20}|pq\rangle \langle o|J_{20}|p'q'\rangle \langle o|J_{20}|pp'\rangle \langle o|J_{20}|qq'\rangle}{(E_p+E_q)(E_p+E_{p'})(E_q+E_{q'})} \right\}$$

We notice first that the constraint $p \neq q \neq p' \neq q'$ can be dropped because the additional terms thus created will cancel each other. Secondly, the third term may be made equal to the second term by exchanging p' with q'. It then follows

$$C'_\eta(4QP) = \tfrac{1}{2}\sum_{\substack{(pq)\pm1\\(p'q')\pm1}} \frac{\langle o|J_{20}|pq\rangle^2 \langle o|J_{20}|p'q'\rangle^2}{(E_p+E_q)^2 (E_{p'}+E_{q'})}$$

$$-\tfrac{1}{2}\sum_{\substack{(pq)\pm1\\(p'q')\pm1}} \frac{\langle o|J_{20}|pq\rangle \langle o|J_{20}|p'q'\rangle \langle o|J_{20}|pq'\rangle \langle o|J_{20}|p'q\rangle}{(E_p+E_q)(E_{p'}+E_{q'})(E_p+E_{q'})(E_{p'}+E_q)} \times \qquad \text{(A.3)}$$

$$\times \quad (E_p+E_{p'}+E_q+E_{q'})$$

The first term in this equation obviously cancels the second term in Eq. (7); we thus defined the full contributions of the four-quasiparticle excitations as

$$C_\eta\,(4QP) = C'_\eta\,(4QP) + \text{second term of Eq. (7)}$$

$$= \text{second term of (A.3)}$$

The summation of the second term in Eq. (A.3) can be separated into four terms

$$\sum_{\substack{(pq)\pm 1\\(p'q')\pm 1}} = \sum_{(pq)_1 (p'q')_1} + \sum_{(pq)_1 (p'q')_{-1}} + \sum_{(pq)_{-1} (p'q')_1} + \sum_{(pq)_{-1} (p'q')_{-1}}$$

The first term yields

$$\sum_{(pq)_1 (p'q')_1} = -\tfrac{1}{2} \sum_{\substack{m_p=\pm 1/2,\pm 3/2,\dots\\ m_{p'}=m_p\\ m_q=m_{q'}=-m_p+1}} \sum_{t_p,t_{p'},t_q,t_{q'}} \frac{\langle o|J_{20}|pq\rangle \langle o|J_{20}|p'q\rangle \langle o|J_{20}|pq'\rangle\langle o|J_{20}|p'q\rangle}{(E_p+E_q)(E_{p'}+E_{q'})(E_p+E_{q'})(E_{p'}+E_q)} \times (E_p+E_{p'}+E_q+E_{q'})$$

$$= -\sum_{\substack{m_p=\pm 1/2,\pm 3/2,\dots\\ m_{p'}=m_p\\ m_q=-m_p+1}} \sum_{t_p,t_{p'}} (E_p+E_{p'}) \left\{ \sum_{t_q} \frac{\langle o|J_{20}|pq\rangle \langle o|J_{20}|p'q\rangle}{(E_p+E_q)(E_{p'}+E_q)} \right\}^2$$

where we have applied the conditions

$$m_p + m_{q'} = \pm 1, \qquad m_{p'} + m_q = \pm 1 \quad .$$

The other three terms can be evaluated in a similar way, and we obtain finally

$$C_\eta(4QP) = -4 \sum_{\substack{m_p>0 \\ m_q=-m_p+1 \\ m_{q'}=-m_p-1}} \sum_{t_q,t_{q'}} (E_q+E_{q'}) \left[\sum_{t_p} \frac{\langle o|J_{20}|pq\rangle \langle o|J_{20}|pq'\rangle}{(E_p+E_q)(E_p+E_{q'})} \right]^2$$

$$-2 \sum_{m_{p'}=m_p>0} \sum_{t_p,t_{p'}} (E_p+E_{p'}) \left[\sum_{\substack{t_q \\ m_q=-m_p\pm1}} \frac{\langle o|J_{20}|pq\rangle \langle o|J_{20}|p'q\rangle}{(E_p+E_q)(E_{p'}+E_q)} \right]^2 . \tag{A.4}$$

Substitution of Eq. (A.2) into Eq. (A.4) then yields the first two terms in Eq. (23).

The contribution of the two-quasiparticle excitations to the first term in Eq. (7) is

$$C_\eta(2QP) = 1/8 \cdot 2 \sum_{\substack{(pq)\pm1 \\ (p'q')0,\pm2 \\ (p_1q_1)\pm1}} \frac{\langle o|J_{20}|pq\rangle \langle pq|J_{11}|p'q'\rangle \langle p'q'|J_{11}|p_1q_1\rangle}{(E_p+E_q)(E_{p'}+E_{q'})} \times \frac{\langle p_1q_1|J_{20}|o\rangle}{(E_{p_1}+E_{q_1})}$$

Since

$$\langle pq|J_{11}|p'q'\rangle = \delta_{pp'}\langle q|J_{11}|q'\rangle + \delta_{qq'}\langle p|J_{11}|p'\rangle - \delta_{pq'}\langle q|J_{11}|p'\rangle - \delta_{qp'}\langle p|J_{11}|q'\rangle$$

one obtains

$$C_\eta\,(2QP) = 2 \sum_{\substack{(pq)\pm 1 \\ (pq')0,\pm 2 \\ (pq_1)\pm 1}} \frac{\langle o|J_{20}|pq\rangle \langle q|J_{11}|q'\rangle \langle q'|J_{11}|q_1\rangle \langle pq_1|J_{20}|o\rangle}{(E_p+E_q)(E_p+E_{q'})(E_p+E_{q_1})}$$

$$+2 \sum_{\substack{(pq)\pm 1 \\ (pq')0,\pm 2 \\ (p'q')\pm 1}} \frac{\langle o|J_{20}|pq\rangle \langle q|J_{11}|q'\rangle \langle p|J_{11}|p'\rangle \langle p'q'|J_{20}|o\rangle}{(E_p+E_q)(E_p+E_{q'})(E_{p'}+E_{q'})} .$$

Recalling that J_x only operates between states with J_z components differed by ± 1, we get

$$C_\eta\,(2QP) = \left\{ 4 \sum_{\substack{(pq)_1 \\ (pq')_0 \\ (pq_1)_1}} + 4 \sum_{\substack{(pq)_1 \\ (pq')_0 \\ (pq_1)_{-1}}} + 4 \sum_{\substack{(pq)_1 \\ (pq')_2 \\ (pq_1)_1}} \right\} \times$$

$$\times \left(\frac{\langle o|J_{20}|pq\rangle \langle q|J_{11}|q'\rangle \langle q'|J_{11}|q_1\rangle \langle pq_1|J_{20}|o\rangle}{(E_p+E_q)(E_p+E_{q'})(E_p+E_{q_1})} \right)$$

$$+ \left\{ 4 \sum_{\substack{(pq)_1 \\ (pq')_0 \\ (p'q')_1}} + 4 \sum_{\substack{(pq)_1 \\ (pq')_0 \\ (p'q')_{-1}}} + \sum_{\substack{(pq)_1 \\ (pq')_2 \\ (p'q')_1}} \right\} \times$$

$$\times \left(\frac{\langle o|J_{20}|pq\rangle \langle q|J_{11}|q'\rangle \langle p|J_{11}|p'\rangle \langle p'q'|J_{20}|o\rangle}{(E_p+E_q)(E_q+E_{q'})(E_{p'}+E_{q'})} \right) \qquad (A.5)$$

where we have used the concise notation

$$\{\Sigma_1 + \Sigma_2 + \Sigma_3\}(A) = \Sigma_1 A + \Sigma_2 A + \Sigma_3 A \quad .$$

We regroup the third and the sixth term in Eq. (A.5) where the J_z components of the two-quasiparticle intermediate states are $m_p + m_{q'} = 2$, and obtain

$$C'_\eta(2QP) = 4 \sum_{\substack{m_p=\pm 1/2,\pm 3/2,\ldots \\ m_{q'}=-m_p+2}} \sum_{t_p,t_{q'}} \frac{1}{E_p+E_{q'}} \left[\sum_{\substack{t_q \\ m_q=-m_p+1}} \frac{\langle o|J_{20}|pq\rangle \langle q|J_{11}|q'\rangle}{E_p+E_q} \right]^2$$

$$+ 4 \sum_{\substack{m_p=\pm 1/2,\pm 3/2,\ldots \\ m_{q'}=-m_p+2}} \sum_{t_p,t_{q'}} \frac{1}{E_p+E_{q'}} \left[\sum_{\substack{t_q \\ m_q=-m_p+1}} \frac{\langle o|J_{20}|pq\rangle \langle q|J_{11}|q'\rangle}{E_p+E_q} \right] \cdot$$

$$\cdot \left[\sum_{\substack{t_q \\ m_q=m_p-1}} \frac{\langle o|J_{20}|qq'\rangle \langle p|J_{11}|q\rangle}{E_{q'}+E_q} \right]$$

The above expression can be rewritten finally as

$$C'_\eta(2QP) = 4 \sum_{\substack{m_p \geq 3/2 \\ m_{q'}=-m_p+2}} \sum_{t_p,t_{q'}} \frac{1}{E_p+E_{q'}} \cdot \left[\sum_{\substack{t_p \\ m_q=-m_p+1}} \frac{\langle o|J_{20}|pq\rangle \langle q|J_{11}|q'\rangle}{E_p+E_q} + \sum_{\substack{t_q \\ m_q=m_p-1}} \frac{\langle o|J_{20}|qq'\rangle \langle p|J_{11}|q\rangle}{E_{q'}+E_q} \right]^2 . \quad (A.6)$$

We then regroup the remaining four terms in Eq. (A.5) where the J_z components of the two-quasiparticle intermediate states are $m_p+m_{q'}=0$, and obtain

$$C''_\eta(2QP) = 4 \sum_{\substack{m_p=\pm1/2,\pm3/2,\ldots \\ m_{q'}=-m_p}} \sum_{t_p,t_{q'}} \frac{1}{E_p+E_{q'}} \left\{ \left[\sum_{\substack{t_q \\ m_q=-m_p+1}} \frac{\langle o|J_{20}|pq\rangle \langle q|J_{11}|q'\rangle}{E_p+E_q} \right]^2 \right.$$

$$+ \left[\sum_{\substack{t_q \\ m_q=-m_p+1}} \frac{\langle o|J_{20}|pq\rangle \langle q|J_{11}|q'\rangle}{E_p+E_q} \right] \left[\sum_{\substack{t_q \\ m_q=-m_p-1}} \frac{\langle o|J_{20}|pq\rangle \langle q|J_{11}|q'\rangle}{E_p+E_q} \right]$$

$$+ \left[\sum_{\substack{t_q \\ m_q=-m_p+1}} \frac{\langle o|J_{20}|pq\rangle \langle q|J_{11}|q'\rangle}{E_p+E_q} \right] \left[\sum_{\substack{t_q \\ m_q=m_p+1}} \frac{\langle o|J_{20}|qq'\rangle \langle p|J_{11}|q\rangle}{E_q+E_{q'}} \right]$$

$$\left. + \left[\sum_{\substack{t_q \\ m_q=-m_p+1}} \frac{\langle o|J_{20}|pq\rangle \langle q|J_{11}|q'\rangle}{E_p+E_q} \right] \left[\sum_{\substack{t_q \\ m_q=m_p-1}} \frac{\langle o|J_{20}|qq'\rangle \langle p|J_{11}|q\rangle}{E_q+E_{q'}} \right] \right\}$$

which can be rewritten finally as

$$C''_\eta(2QP) = 2 \sum_{\substack{m_p>0 \\ m_{q'}=-m_p}} \sum_{t_p,t_{q'}} \frac{1}{E_p+E_{q'}} \left[\sum_{\substack{t_q \\ m_q=-m_p\pm1}} \frac{\langle o|J_{20}|pq\rangle \langle q|J_{11}|q'\rangle}{E_p+E_q} + \sum_{\substack{t_q \\ m_q=m_p\pm1}} \frac{\langle o|J_{20}|qq'\rangle \langle q|J_{11}|p\rangle}{E_q+E_{q'}} \right]^2 \tag{A.7}$$

Substitution of Eq. (A.2) into Eqs. (A.6) and (A.7) then yields the last two terms in Eq. (23).

FOOTNOTES AND REFERENCES

* Work performed under the auspices of the U. S. Atomic Energy Commission.

+ Present address: Physics Department and Cyclotron Institute, Texas A&M University, College Station, Texas 77843.

1. R. A. Sorensen, Rev. Mod. Phys. 45, 353 (1973).

2. A. Johnson and Z. Szymanski, Phys, Reports 7C, 182 (1973).

3. A. Johnson, H. Ryde, and S. A. Jyorth, Nucl. Phys. A179, 753 (1972); A. Johnson, H. Ryde, and J. Starkier, Phys. Lett. 34B, 605 (1971).

4. R. M. Diamond, F. S. Stephens and W. J. Swiatecki, Phys. Letters 11, 315 (1964).

5. P. C. Sood, Can. J. Phys. 46, 1419 (1968); Nucl. Data A4, 281 (1968).

6. S. M. Harris, Phys. Rev. 138, 509 (1965).

7. M. A. J. Mariscotti, G. Scharff-Goldhaber and B. Buck, Phys, Rev. 178, 1864 (1969).

8. J. E. Draper, Phys. Letters 41B, 105 (1972).

9. T. K. Das and B. Banerjee, Phys, Rev. C7, 2590 (1973).

10. A. Goodman and A. Goswami, Phys. Rev. C9, 1948 (1974).

11. T. Udagawa and R. K. Sheline, Phys. Rev. 147, 671 (1966).

12. K. Y. Chan and J. G. Valatin, Nucl. Phys. 82, 222 (1966); K. Y. Chan, ibid. 85, 261 (1966).

13. D. R. Bes, S. Landowne and M. A. J. Mariscotti, Phys, Rev. 166, 1045 (1968).

14. M. Sano and M. Wakai, Nucl. Phys. A97, 298 (1967); Prog. Theor. Phys. 47, 880 (1972).

15. J. Krumlinde, Nucl. Phys. A121, 306 (1968); A160, 471 (1971).

16. E. R. Marshalek, Phys. Rev. 139, B770 (1965); 158, 993 (1967), Phys. Rev. Letters 20, 214 (1968).

17. C. W. Ma and J. O. Rasmussen, Phys. Rev. C 2, 798 (1970).

18. B. R. Mottelson and J. G. Valatin, Phys. Rev. Letters 5, 511 (1960).

19. K. Kumar, Physica Scripta 6, 270 (1972); Phys. Rev. Lett. 30, 1227 (1973).

20. A. Faessler, L. Lin and F. Wittmann, Phys. Letters 44B, 127 (1973); A. Faessler, F. Grummer, L. Lin and J. Urbano, Phys. Lett. 48B, 87 (1974).

21. H. R. Dalafi, B. Banerjee. H. J. Mang and P. Ring, Phys. Letters 44B, 327 (1973); B. Banerjee, H. J. Mang, and P. Ring, Nucl. Phys. A215, 366 (1973).

22. D. R. Inglis, Phys. Rev. 96, 1059 (1954); 103, 1786 (1956).

23. S. G. Nilsson, C. F. Tsang, A. Sobiczewski, Z. Szymanski, S. Wycech, C. Gustafson, I. L. Lamm, P. Moller and B. Nilsson, Nucl, Phys. A131, 1 (1969).

24. A. Klein, R. M. Dreizler and T. K. Das, Phys. Letters 31B, 33 (1970).

25. O. Saethre, S. A. Hjorth, A. Johnson, S. Jagare, H. Ryde and Z. Szymanski, Nucl. Phys. A207, 486 (1973).

26. S. T. Belyaev, Kgl. Danske Videnskab Selskab, Mat-Fys. Medd. 31, No. 11 (1959).

27. J. Meyer, J. Speth, J. H. Vogeler, Nucl. Phys. A193, 60 (1972).

28. M. Rich, Nucl. Phys. A90, 407 (1967).

29. J. Bang, J. Krumlinde and S. G. Nilsson, Phys. Letters 15, 55 (1965).

30. J. F. Goodfellow and Y. Nogami, Can. J. Phys. 44, 1321 (1966).

31. S. G. Nilsson and O. Prior, Kgl. Danske Videnskab Selskab, Mat.-Fys. Medd. 32, No. 16 (1961).

32. R. M. Diamond, G. D. Symons, J. L. Quebert, K. H. Maier, J. R. Leigh and F. S. Stephens, Nucl. Phys. A184, 481 (1972).

33. W. Ogle, S. Wahlborn, R. Piepenbring and S. Fredricksson, Rev. Mod. Phys. 43, 424 (1971).

34. A. Sobiczewski, S. Bjørnholm, and K. Pomorski, Nucl. Phys. A202, 274 (1973).

Table I. The quadrupole and hexadecapole deformation parameters ε_2 and ε_4 are taken from Ref. 23. The energy gap Δ_p and Δ_n are calculated with pairing strength G as given in Eq. (11).

Nucleus	ε_2	ε_4	Δ_p (MeV)	Δ_n (MeV)
Sm 152	0.202	-0.036	1.114	0.975
154	0.227	-0.039	1.024	0.888
Gd 154	0.206	-0.029	1.101	1.001
156	0.233	-0.030	1.020	0.935
158	0.245	-0.024	0.980	0.895
160	0.255	-0.015	0.948	0.849
Dy 160	0.245	-0.015	0.988	0.934
162	0.256	-0.006	0.945	0.880
164	0.264	0.003	0.910	0.836
Er 162	0.242	-0.007	0.989	0.969
164	0.254	0.001	0.941	0.906
166	0.261	0.010	0.898	0.861
168	0.272	0.020	0.847	0.815
170	0.273	0.031	0.807	0.786
Yb 166	0.246	0.004	1.002	0.926
168	0.255	0.014	0.956	0.883
170	0.265	0.025	0.902	0.835
172	0.270	0.037	0.845	0.799
174	0.266	0.048	0.799	0.739
176	0.258	0.053	0.785	0.661
Hf 174	0.258	0.034	0.915	0.822
176	0.256	0.043	0.879	0.734
178	0.250	0.052	0.844	0.672
180	0.243	0.063	0.808	0.561
W 180	0.236	0.050	0.870	0.699
182	0.232	0.060	0.828	0.602
184	0.216	0.061	0.793	0.735
186	0.197	0.060	0.777	0.790
Os 184	0.213	0.053	0.750	0.690
186	0.198	0.055	0.665	0.780
188	0.178	0.055	0.592	0.819

Table II. The moment-of-inertia and the inertia derivatives, where $D_{xi} \equiv \left[\frac{\partial}{\partial x_i}(2J_o/\hbar^2)\right]_{x_{io}}$.

Nucleus	$D_{\varepsilon 2}$ (MeV^{-1})	$D_{\varepsilon 4}$ (MeV^{-1})	$D_{\nu p}$ (MeV^{-2})	$D_{\nu n}$ (MeV^{-2})	$2J_p/\hbar^2$ (MeV^{-1})	$2J_n/\hbar^2$ (MeV^{-1})	$2J_o/\hbar^2$ (MeV^{-1})	$2J_{exp}/\hbar^2$ (MeV^{-1})
Sm 152	196	-266	-16.68	-32.35	13.62	24.84	40.38	46.8
154	163	-266	-20.17	-46.17	17.16	35.19	54.97	73.0
Gd 154	195	-236	-15.51	-29.85	13.26	23.14	38.22	46.6
156	168	-235	-18.49	-41.16	16.33	32.00	50.75	66.6
158	119	-176	-19.88	-37.59	17.45	33.27	53.26	74.8
160	126	-150	-20.98	-40.19	18.20	35.40	56.28	79.4
Dy 160	131	-169	-19.48	-35.24	16.55	30.63	49.53	68.6
162	126	-137	-20.55	-38.17	17.60	33.33	53.48	73.8
164	94	-116	-21.25	-43.05	18.33	35.84	56.88	81.2
Er 162	148	-147	-16.15	-32.72	15.07	27.99	45.21	58.6
164	134	-109	-17.25	-36.35	16.38	31.41	50.17	65.4
166	102	-87	-18.22	-41.23	17.41	34.00	53.98	73.8
168	85	-35	-19.04	-36.48	18.74	35.11	56.54	75.0
170	108	4	-19.93	-40.27	19.59	36.77	59.19	75.6
Yb 166	154	-86	-14.94	-35.08	14.16	29.59	45.94	57.8
168	135	-68	-16.52	-39.72	15.54	32.27	50.20	68.4
170	118	-19	-18.14	-36.34	17.20	33.76	53.51	70.8
172	124	7	-19.70	-39.98	18.75	35.96	57.45	75.8
174	89	-4	-21.11	-41.15	19.78	36.83	59.44	78.4
176	49	11	-21.87	-31.59	19.90	35.45	58.12	72.8
Hf 174	141	-11	-13.18	-37.80	14.90	34.40	51.77	65.4
176	108	-17	-13.38	-45.53	15.38	38.19	56.25	67.6
178	53	-7	-13.68	-35.14	15.74	36.42	54.77	64.0
180	15	35	-13.88	-33.54	16.18	39.02	57.96	64.2
W 180	63	3	-3.69	-36.56	12.34	35.26	49.98	57.6
182	21	52	-8.94	-35.55	12.90	37.84	53.28	59.6
184	69	65	-9.91	-28.92	12.88	31.00	46.07	53.6
186	89	74	-10.87	-22.25	12.55	24.76	39.18	48.6
Os 184	49	62	-9.25	-36.92	11.92	34.35	48.58	49.4
186	79	68	-10.75	-29.99	12.62	28.53	43.20	43.0
188	86	68	-12.97	-22.67	13.29	22.64	37.72	37.4

Table III. The spring constants associated with various degrees of freedom.

Nucleus	C_{22} (MeV)	C_{44} (MeV)	$C_{\nu p}$ (MeV^{-1})	$C_{\nu n}$ (MeV^{-1})	C_{η} (MeV^{-3})
Sm 152	760	1205	3.67	3.88	27.32
154	966	1519	3.74	3.27	37.68
Gd 154	725	1222	3.72	3.93	23.61
156	899	1453	3.75	3.50	31.48
158	1019	1556	3.78	4.18	24.81
160	1092	1620	3.81	4.13	28.44
Dy 160	989	1450	3.36	4.18	23.79
162	1108	1592	3.36	4.19	27.36
164	1215	1711	3.40	3.50	33.25
Er 162	926	1318	3.73	4.22	19.27
164	1043	1503	3.66	4.24	22.38
166	1175	1663	3.62	3.59	27.44
168	1205	1780	3.58	4.40	17.75
170	1181	2005	3.57	4.18	23.34
Yb 166	956	1390	3.93	4.27	21.21
168	1064	1517	3.83	3.69	26.56
170	1097	1645	3.66	4.40	19.49
172	1113	1714	3.46	4.25	25.66
174	1220	1710	3.34	4.03	30.56
176	1275	1709	3.39	5.20	19.89
Hf 174	1032	1637	4.10	4.56	20.90
176	1178	1643	4.20	3.71	31.15
178	1243	1603	4.29	4.92	21.16
180	1300	1600	4.39	2.19	14.27
W 180	1238	1600	4.15	4.76	18.34
182	1280	1595	4.18	2.49	12.16
184	1255	1450	4.37	5.25	15.29
186	1175	1225	4.60	5.37	12.46
Os 184	1280	1663	2.45	3.06	13.53
186	1225	1488	2.06	5.14	16.28
188	1188	1325	1.77	5.36	13.12

TABLE IV. The first four columns list pairing spring constants with and without fixed-particle-number correction (PBCS and BCS). The fifth and sixth columns give separately the two and four quasiparticle contributions to the fourth-order cranking constant.

Nucleus	$C_{\nu p}$ (MeV^{-2})		$C_{\nu n}$ (MeV^{-2})		C_{η} (MeV^{-3})	
	BCS	PBCS	BCS	PBCS	2Q.P.	4Q.P.
^{154}Sm	3.17	3.74	3.07	3.27	49.8	-12.2
^{158}Gd	3.21	3.78	3.43	4.18	35.2	-10.4
^{162}Dy	3.07	3.36	3.50	4.19	37.7	-10.4
^{166}Er	3.09	3.62	3.36	3.59	37.7	-10.3
^{170}Yb	3.18	3.66	3.60	4.40	28.8	-9.35
^{174}Hf	3.44	4.10	3.70	4.56	30.0	-9.06
^{180}W	3.32	4.15	3.40	4.76	27.3	-8.97
^{184}Os	2.45	2.45	2.89	3.06	22.3	-8.76

TABLE V. The force constant C_{VMI}^{-1} and the separate contributions from various higher order effects. The experimental values of C_{VMI}^{-1} are taken from Ref. 7. We define $K_{xi} \equiv \left(\frac{\partial}{\partial x_i} J_o/\hbar^2\right)^2/C_i$. All units are in MeV^{-3}.

Nucleus	K_{22}	K_{44}	$K_{\nu p}$	$K_{\nu n}$	$4C_H$	C_{VMI}^{-1} (Calc.)	C_{VMI}^{-1} (exp.)
Sm152	13	15	18.98	67.45	109.53	224.0	595
154	7	12	27.20	163.11	150.73	353.0	229
Gd154	13	11	16.16	56.68	94.46	191.3	544
156	8	10	22.78	121.15	125.94	287.9	338
158	3	5	26.13	84.55	99.24	217.9	245
160	4	4	28.85	97.89	113.76	248.5	215
Dy160	4	5	28.25	74.28	95.15	206.7	219
162	4	3	31.43	86.97	109.44	234.8	195
164	2	2	33.23	132.55	132.99	302.8	238
Er162	6	4	17.48	63.43	77.07	168.0	255
164	4	2	20.29	77.95	89.50	193.7	197
166	2	1	22.96	118.26	109.76	254.0	240
168	2	0	25.35	75.57	70.98	173.9	110
170	2	0	27.80	96.92	93.36	220.1	132
Yb166	6	2	14.19	71.98	84.83	179.0	255
168	4	1	17.79	106.91	106.23	235.9	258
170	3	0	22.48	75.03	77.96	178.5	160
172	3	0	28.05	93.90	102.64	227.6	213
174	2	0	33.33	105.01	122.26	262.6	108
176	0	0	35.23	48.01	79.57	162.8	128
Hf174	5	0	10.60	78.40	83.61	177.6	215
176	2	0	10.66	139.57	124.61	276.8	170
178	1	0	10.90	62.80	84.66	159.4	135
180	0	0	10.97	128.56	57.06	196.6	73
W180	1	0	4.55	70.13	73.35	149.1	188
182	0	0	4.79	126.76	48.65	180.2	98
184	1	1	5.61	39.81	61.16	108.6	102
186	2	1	6.42	23.04	49.84	82.3	93
Os184	1	1	8.74	111.23	54.14	176.1	180
186	1	1	14.04	43.71	65.11	124.9	162
188	2	1	23.82	23.96	52.49	103.3	196

Table VI. The results of calculation B where neutron levels have been shifted according to Eq. (24).

Nucleus	$\Delta\eta$ (MeV)	$\frac{\partial}{\partial\nu_n}\left(\frac{2J_o}{\hbar^2}\right)$ (MeV^{-2})	$C_{\nu n}$ (MeV^{-1})	C_η (MeV^{-3})	$\frac{2J_n}{\hbar^2}$ (MeV^{-1})	$\frac{2J_o}{\hbar^2}$ (MeV^{-1})	C^{-1}_{VMI} (MeV^{-3})	$-B_{theo}$ (eV)	$-B_{exp}$ (eV)
Sm152	0.975	-32.35	3.88	27.32	24.84	40.38	224.0	169	195
154	0.888	-46.17	3.27	37.68	35.19	54.97	353.0	77.3	14.9
Gd154	1.001	-29.85	3.93	23.61	23.14	38.22	191.3	179	180
156	0.935	-41.16	3.50	31.48	32.00	50.75	287.9	86.8	33.8
158	0.895	-37.59	4.18	24.81	33.27	53.26	217.9	54.2	17.5
160	0.849	-40.19	4.13	28.44	35.40	56.28	248.5	49.5	11.8
Dy160	0.934	-35.24	4.18	23.79	30.63	49.53	206.7	68.7	20.7
162	0.880	-38.17	4.19	27.36	33.33	53.48	234.8	57.4	12.0
164	0.836	-43.05	3.50	33.25	35.84	56.88	302.8	57.9	12.0
Er162	0.969	-32.72	4.22	19.27	27.99	45.21	168.0	80.4	40.0
164	0.906	-36.35	4.24	22.38	31.41	50.17	193.7	61.1	19.9
166	0.861	-41.23	3.59	27.44	34.00	53.98	254.0	59.8	17.4
168	0.815	-36.48	4.40	17.75	35.11	56.54	173.9	34.0	6.74
170	0.771	-44.06	3.48	25.57	38.84	58.43	271.7	46.6	10.1
Yb166	0.926	-35.08	4.27	21.21	29.59	45.94	179.0	80.4	49.5
168	0.883	-39.72	3.69	26.56	32.27	50.20	235.9	74.3	22.9
170	0.813	-37.41	4.38	19.58	35.34	52.54	183.8	48.2	12.7
172	0.786	-43.59	3.61	27.80	37.86	56.61	273.9	53.3	10.4
174	0.789	-36.41	4.70	26.46	34.99	54.78	211.6	50.0	5.79
176	0.746	-29.64	4.95	17.55	33.14	53.05	149.8	37.8	12.9

(continued)

Table VI. continued

Nucleus	Δ_n (MeV)	$\frac{\partial}{\partial \nu_n}\left(\frac{2J_o}{\hbar^2}\right)$ (MeV^{-2})	$C_{\nu n}$ (MeV^{-1})	C_η (MeV^{-3})	$\frac{2J_n}{\hbar^2}$ (MeV^{-1})	$\frac{2J_o}{\hbar^2}$ (MeV^{-1})	C_{VWI}^{-1} (MeV^{-3})	$-B_{theo}$ (eV)	$-B_{exp}$ (eV)
Hf174	0.825	-41.11	3.98	22.85	35.61	50.51	213.2	65.5	21.0
176	0.803	-39.93	4.42	26.53	35.30	50.68	298.9	63.3	14.7
178	0.770	-32.51	4.62	18.10	33.19	48.93	141.5	49.4	15.1
180	0.721	-30.89	3.68	13.82	33.48	49.65	131.0	43.1	6.36
W 180	0.795	-33.53	4.55	15.19	31.88	44.23	128.1	66.9	39.9
182	0.747	-31.94	3.84	11.13	32.48	45.38	115.7	54.6	16.8
184	0.749	-31.75	4.75	14.65	31.09	43.98	119.2	63.7	24.4
186	0.759	-27.90	4.78	14.91	26.98	39.54	109.8	89.8	34.2
Os184	0.807	-32.37	4.08	11.75	29.71	41.63	121.9	81.2	59.2
186	0.809	-31.47	4.76	15.16	27.93	40.55	128.7	95.2	88.2
188	0.814	-26.63	5.09	14.92	23.84	37.13	121.3	128	174

TABLE VII. The moment-of-inertia, B coefficient and the force constant calculated with g_o = 18.0 MeV in Eq. (11), the results of Marshalek[16] are also listed for comparison.

Nucleus	This Calculation			Marshalek	
	$\frac{2Jo}{\hbar^2}$ (MeV^{-1})	-B (ev)	C^{-1}_{VMI} (MeV^{-3})	$\frac{2Jo}{\hbar^2}$ (MeV^{-1})	-B (ev)
Sm152	55.57	99.8	476	46.77	221
154	78.02	50.4	934	72.31	37.5
Gd154	52.17	109	403	46.30	160
156	70.69	56.9	711	66.53	43.0
158	69.66	32.4	382	74.96	26.7
160	73.42	29.4	427	79.05	25.4
Dy160	66.06	42.7	407	68.45	37.4
162	70.74	34.6	433	74.02	33.4
164	78.00	39.6	733	81.37	26.0
Er164	65.54	36.9	340	65.19	43.7
166	73.17	43.5	623	73.96	33.7
168	71.40	19.3	251	74.96	25.0
170	75.56	21.2	346	75.13	30.0
Yb170	68.33	25.5	278	70.82	31.8
172	73.90	25.0	373	75.93	30.0
174	76.61	28.1	485	77.82	27.8
176	71.03	20.8	265	72.46	27.7
Hf176	73.30	39.5	570	67.43	42.6
178	66.44	26.1	254	64.10	44.0
W 184	54.67	29.8	133	53.48	68.5
186	46.41	50.4	117	48.40	99.1

FIGURE CAPTIONS

Fig. 1. The moment-of-inertia $J_o/\hbar^2$. The theoretical values are calculated with the single particle states and pairing strength (Eq. (11)) as given by Nilsson et al.[23] The experimental values are taken from Mariscotti et al.[7]

Fig. 2. The force constant C_{VMI}^{-1}. The theoretical values are calculated with the single particle states and pairing strength (Eq. (11)) as given in Nilsson et al.[23] The experimental values are taken from Mariscotti et al.[7] Note the large discrepancies at neutron number N = 90, 104 and 108.

Fig. 3. Same as Fig. 2, except in these calculations the neutron levels have been shifted according to Eq. (24).

Fig. 4. The B-coefficient. The theoretical values are calculated with the pairing strength as given in Eq. (11) and with the neutron levels shifted according to Eq. (24).

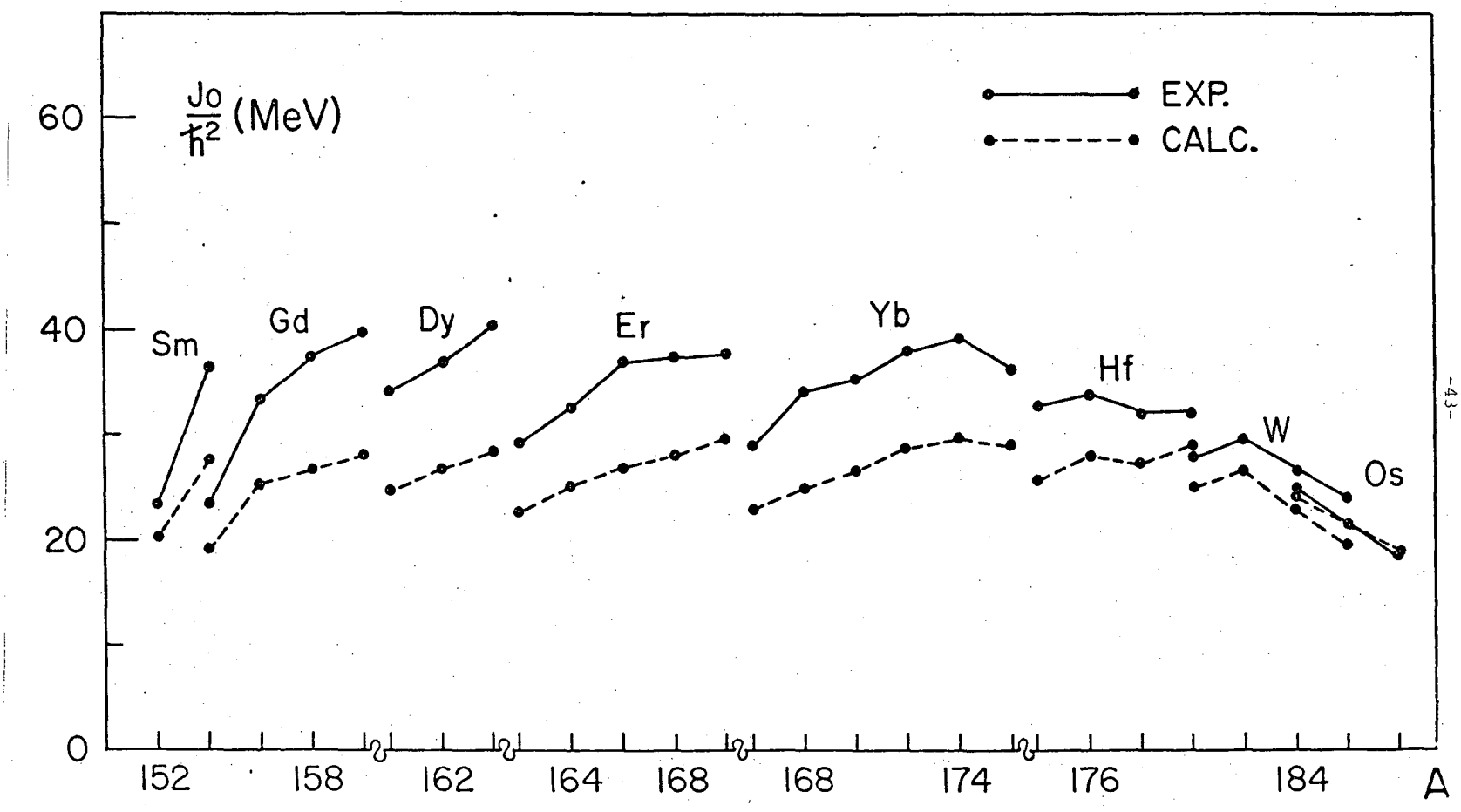

Fig. 1

LBL-2347

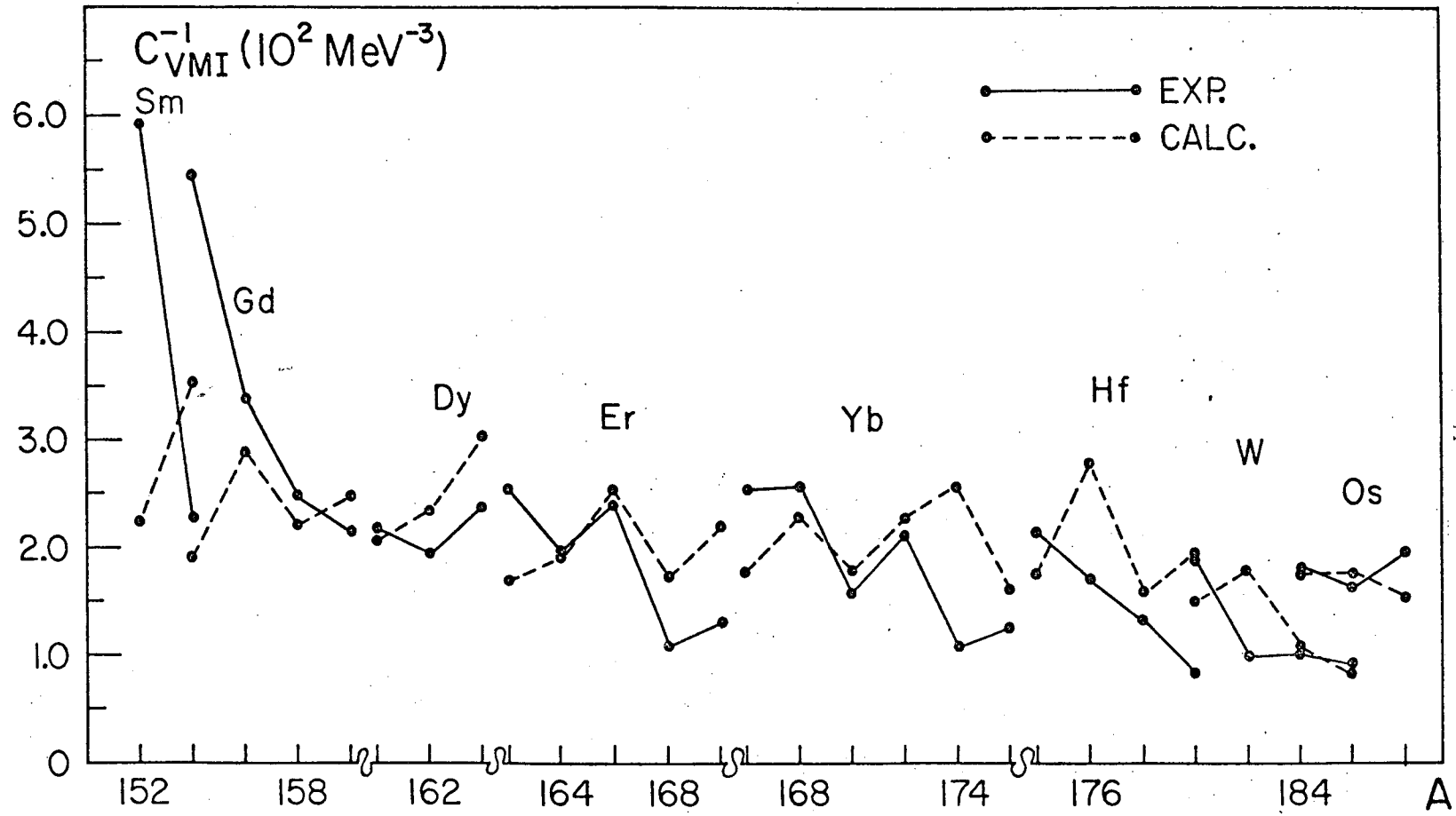

Fig. 2

LBL-2347

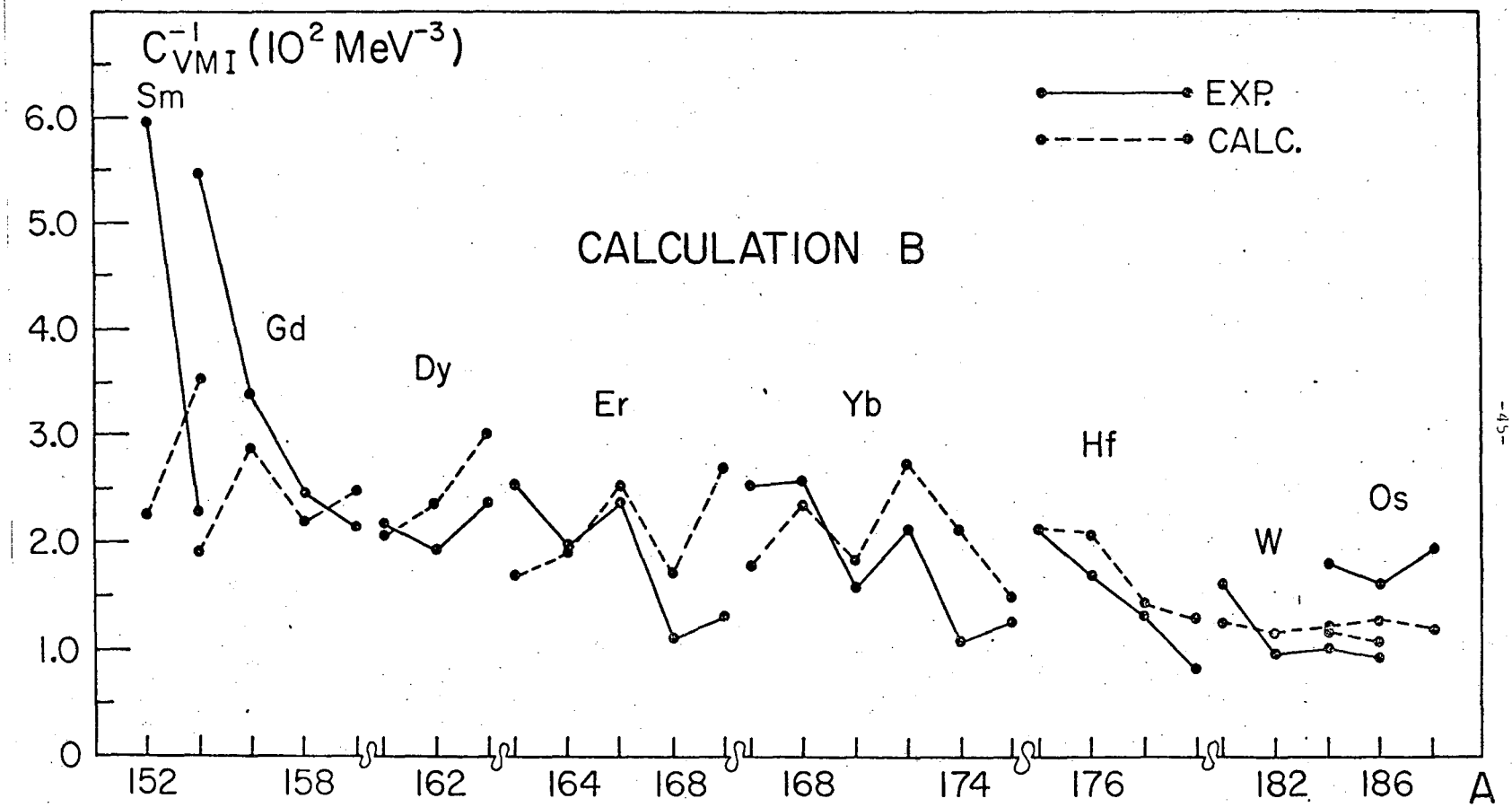

Fig. 3

LBL-2347

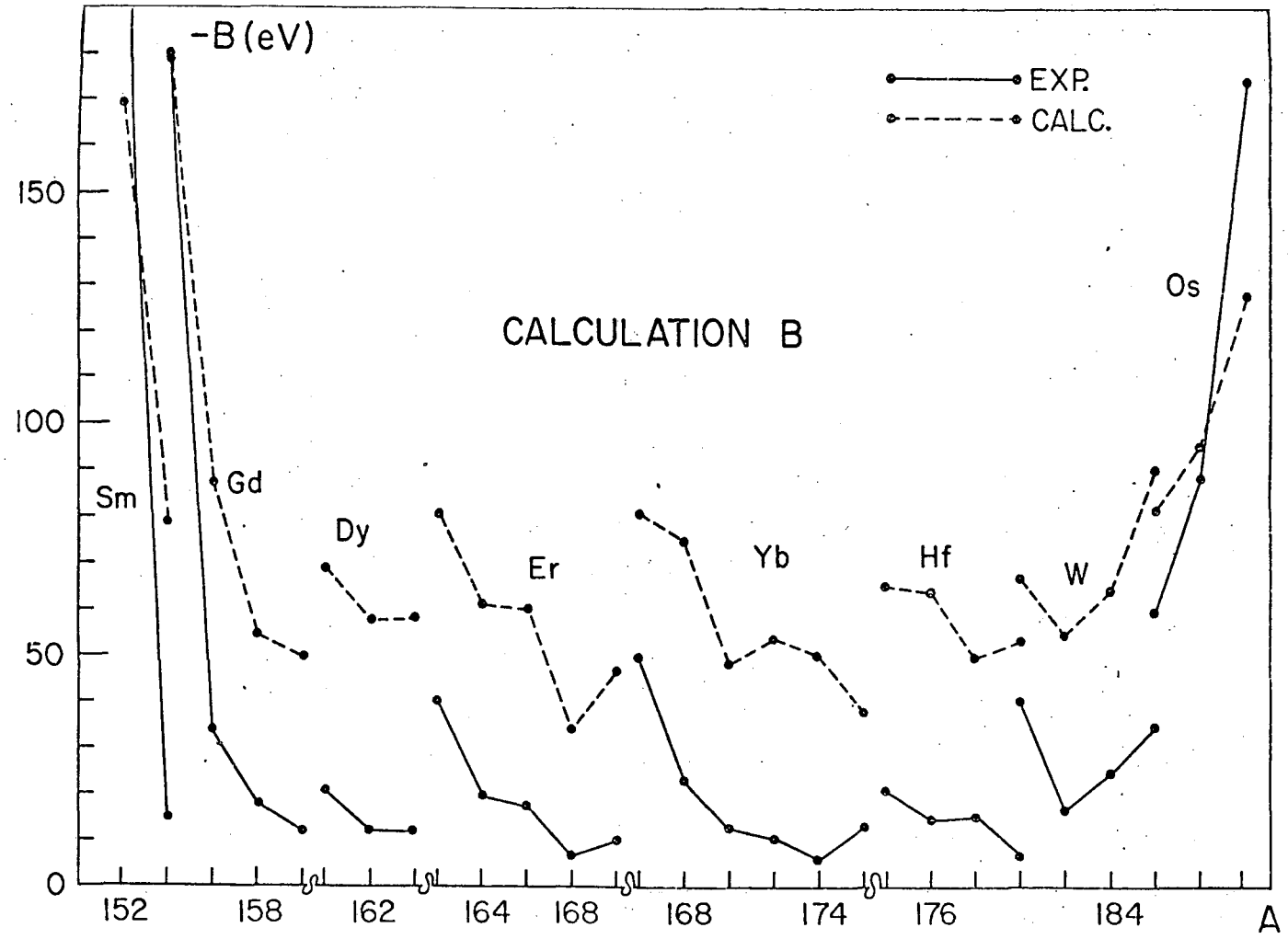

Fig. 4

LBL-2347

TECHNICAL INFORMATION DIVISION
LAWRENCE BERKELEY LABORATORY
UNIVERSITY OF CALIFORNIA
BERKELEY, CALIFORNIA 94720